

# GDF11 Inhibits Bone Formation by Activating Smad2/3 in Bone Marrow Mesenchymal Stem Cells

Qiong Lu<sup>1,2,3,4</sup> · Man-Li Tu<sup>1,2,5</sup> · Chang-Jun Li<sup>1,2</sup> · Li Zhang<sup>1,2</sup> · Tie-Jian Jiang<sup>6</sup> · Tang Liu<sup>7</sup> · Xiang-Hang Luo<sup>1,2</sup> 

Received: 21 March 2016 / Accepted: 30 June 2016 / Published online: 9 July 2016  
© Springer Science+Business Media New York 2016

**Abstract** Growth differentiation factor 11 (GDF11) is a member of the transforming growth factor- $\beta$  superfamily. Recent studies confirmed that GDF11 plays an important role in regulating the regeneration of brain, skeletal muscle, and heart during aging; however, its role in bone metabolism remains unclear. Thus, the aim of this study was to determine the effects of GDF11 on bone metabolism, including bone formation and bone resorption, both in vitro and in vivo. Our results showed that GDF11 inhibited osteoblastic differentiation of bone marrow mesenchymal stem cells in vitro. Mechanistically, GDF11 repressed Runx2 expression by inducing SMAD2/3 phosphorylation during osteoblast differentiation. Moreover, intraperitoneal

injection of GDF11 inhibited bone formation and accelerated age-related bone loss in mice. Our results also showed that GDF11 had no effect on osteoclast differentiation or bone resorption both in vitro and in vivo. These results provide a further rationale for the therapeutic targeting of GDF11 for the treatment of age-related osteoporosis.

**Keywords** Growth differentiation factor 11 · Osteoblast · Aging · Osteoporosis · Bone marrow mesenchymal stem cells

## Introduction

Growth differentiation factor 11 (GDF11), a member of the transforming growth factor- $\beta$  (TGF- $\beta$ ) superfamily, circulates in the bloodstream of mammals [1–4]. GDF-11 is a myostatin homologous protein that acts as an inhibitor of nerve tissue growth. GDF-11 has been shown to suppress neurogenesis through a myostatin-like pathway, which involves arrest of the progenitor cell cycle in the G1 phase. A recent study showed that GDF11 levels were involved in the development of age-related diseases, such as age-related brain and skeletal muscle dysfunctions, and cardiac hypertrophy [1–3, 5]. It has been shown that GDF11 has a regenerative effect on cardiac hypertrophy, skeletal muscle, and brain. GDF11 levels have also been shown to increase with age and to inhibit skeletal muscle regeneration [6]. Thus, the results of these studies highlight that the exact mechanism of action of GDF11 remains unclear. The ability of GDF11 to reverse age-related disorders in other tissues, such as the bone, also remains unknown.

Osteoporosis is defined as a disease that weakens bone structure and increases the risk of fractures [7, 8]. Aging is a major risk factor for osteoporosis, which is becoming a

✉ Xiang-Hang Luo  
xianghangluo@sina.com

<sup>1</sup> Department of Metabolism & Endocrinology, The Second Xiangya Hospital of Central South University, Changsha 410011, Hunan, People's Republic of China

<sup>2</sup> National Clinical Research Center for Metabolic Diseases, The Second Xiangya Hospital of Central South University, Changsha 410011, Hunan, People's Republic of China

<sup>3</sup> Department of Pharmacy, The Second Xiangya Hospital of Central South University, Changsha 410011, Hunan, People's Republic of China

<sup>4</sup> Department of Radiology and Imaging Sciences, Emory University School of Medicine, Atlanta, GA 30322, USA

<sup>5</sup> Department of Orthopaedics Surgery, Johns Hopkins University School of Medicine, Baltimore, MD 21205, USA

<sup>6</sup> Department of Endocrinology, The Xiangya Hospital of Central South University, Changsha 410008, Hunan, People's Republic of China

<sup>7</sup> Department of Orthopaedics Surgery, The Second Xiangya Hospital of Central South University, Changsha 410011, Hunan, People's Republic of China

serious issue in our aging society [9, 10]. The mechanism of osteoporosis in aging persons is unique in terms of the cellular changes and response to osteoporotic treatments. Therefore, it is important to identify the factors that change with aging and that affect the development of osteoporosis [11]. Bone remodeling of osseous tissues comprises a dynamic repetition of bone resorption by osteoclasts and bone synthesis by osteoblasts, and this process is regulated to ensure that a balance is maintained [12]. The balance between osteoblastic bone formation and osteoclastic bone resorption plays an important role in the progress of bone remodeling, which maintains bone homeostasis [13, 14]. Emerging evidence indicates that systemic factors, such as estrogen, oxidants, and other cytokines, profoundly influence bone metabolism and result in age-related bone loss. Identifying potential targets for osteoporosis intervention can have profound socioeconomic significance for public health.

Recently, some studies identified GDF11 as a novel factor affected by osteoporosis and aging. Zhang et al. showed that GDF11 is a protective factor for osteogenesis by inhibiting the activity of the peroxisome proliferator-activated receptor- $\gamma$  [11]. Li et al. showed that antagonism of GDF11 activity in transgenic mice promoted osteoblastic activities and bone formation [15]. Thus, the exact mechanism of action of GDF11 on bone metabolism remains controversial. In particular, the effects of recombinant GDF11 in mice remain unclear.

Although GDF11 levels have been associated with age-related diseases, such as brain and skeletal muscle dysfunctions, and cardiac hypertrophy, they have been no reports of its effects in age-related osteoporosis. The present study was undertaken to elucidate the effects of GDF11 on bone metabolism, including bone formation and bone resorption, both in vitro and in vivo. This study provides new evidence of an association between age-related osteoporosis and GDF11.

## Materials and Methods

### Bone Marrow Mesenchymal Stem Cell (BMSC) Isolation and Culture

Mouse BMSCs were isolated as previously described [16, 17]. In brief, bone marrow cells were flushed from the femurs of female mice and incubated for 20 min at 4 °C with phycoerythrin (PE)-, FITC-, peridinin chlorophyll protein (Per CP)-, and allophycocyanin (APC)-conjugated antibodies, which recognized mouse Sca-1, CD29, CD45, and CD11b (BioLegend). Acquisition was performed using fluorescence-activated cell sorting (FACS) (Aria model; BD Biosciences), and the analysis was performed using the

FACS DIVE software version 6.1.3 (BD Biosciences). The sorted CD29<sup>+</sup>/Sca-1<sup>+</sup>/CD45<sup>-</sup>/CD11b<sup>-</sup> cells were enriched by further culture.

Sorted mouse CD29<sup>+</sup>/Sca-1<sup>+</sup>/CD45<sup>-</sup>/CD11b<sup>-</sup> BMSCs were cultured for 1–2 weeks, until they reached 80–85 % confluence. Then, first-passage BMSCs were detached and seeded in culture flasks for enrichment of cell populations. As second-passage BMSCs reached confluence after approximately 1 week, they were subcultured. Only third-passage BMSCs were subjected to induction of osteogenic differentiation.

### Osteogenic Differentiation and Mineralization Assay

To induce osteoblastic differentiation [16–19], BMSCs were cultured in 24-well plates at a density of  $5 \times 10^5$  cells/well, with osteogenesis induction medium (50  $\mu$ M ascorbic acid, 10 nM dexamethasone, and 10 mM  $\beta$ -glycerophosphate) for 3 days, following which they were treated with 3–30 ng/mL GDF11 (R&D Systems) for 48 h. Then, cell lysates were homogenized for alkaline phosphatase (ALP) activity assay by spectrophotometric measurement of *p*-nitrophenol release using an enzymatic colorimetric ALP Kit (Roche). Culture media were collected for assessment of secreted osteocalcin (OCN) levels using a specific immunoassay kit (DiaSorin).

To induce osteoblastic mineralization, BMSCs were cultured in six-well plates, at a density of  $2.5 \times 10^6$  cells/well, for 21 days using osteogenesis induction medium, as described above. Then, cells were stained with 2 % Alizarin Red S (Sigma-Aldrich) at pH 4.2 to evaluate cell matrix mineralization. A Diaphot Inverted Microscope and Camera System (Nikon) were used for imaging. Alizarin Red S released from the cell matrix into the cetyl-pyridiniumchloride solution was quantified by spectrophotometry at 540 nm. To normalize protein expression levels to total cellular protein, a fraction of the lysate solution was subjected to Bradford assay.

### Osteoclast Culture

Mouse bone marrow cells were cultured on petri dishes in  $\alpha$ -minimal essential medium containing 10 % fetal bovine serum, 100 U/mL penicillin, 100  $\mu$ g/mL streptomycin sulfate, and 30 ng/mL macrophage colony-stimulating factor (M-CSF; R&D Systems Inc.) overnight. After discarding of the adherent cells, floating cells were incubated with M-CSF (30 ng/mL) to obtain monocytes and macrophages. Monocytes and macrophages were further cultured in 24-well plates ( $1 \times 10^5$  cells per well) with 30 ng/mL M-CSF and 200 ng/mL receptor activator of nuclear factor kappa-B ligand (RANKL) for 8 days to obtain mature multinucleated osteoclasts. Tartrate-resistant acid

phosphatase (TRAP) activities of the osteoclasts were detected using a commercial kit (Sigma-Aldrich).

### Experimental Design and Animal Model

Twelve-month-old female C57BL/6 mice were obtained from the Chinese Academy of Science (Shanghai, China) for *in vivo* studies. For recombinant GDF11 treatment, all mice were randomly divided into two groups as follows: control group ( $n = 6$ ) and GDF11-treated group ( $n = 6$ ). Two groups were treated with GDF11 (0.1 mg/kg) or vehicle every day (intraperitoneal injection) for 12 weeks, following which they were anesthetized and euthanized. Femurs were harvested and fixed with 4 % paraformaldehyde for 24 h at 4 °C, then decalcified in 10 % ethylenediaminetetraacetic acid (pH 7.4) for 21 days, before being embedded in paraffin. Four-micrometer-thick longitudinally-oriented bone sections were stained.

### Microcomputed Tomography Analysis

The right femurs and lumbar spines dissected from mice were fixed with 4 % paraformaldehyde for 24 h, then scanned and analyzed with a GE Explore Locus SP microcomputed tomography ( $\mu$ CT) system (GE Healthcare Co.). X-ray voltage and current were set to 65 kV and 165  $\mu$ A, respectively, with a resolution of 8.0  $\mu$ m per pixel. Cross-sectional images of distal femurs and L4 vertebrae were used to perform three-dimensional histomorphometric analysis of trabecular bone. For the distal femur, the region of interest (ROI) selected for analysis was 5 % of the femoral length from 0.1 mm below the growth plate, to determine trabecular bone volume per tissue volume (Tb.BV/TV), trabecular number (Tb.N), trabecular separation (Tb.Sp), and trabecular thickness (Tb.Th). For L4 vertebrae, the entire region of the trabecular bone was selected for analysis to determine the trabecular bone volume per tissue volume (Vt.BV/TV). Cross-sectional images of the mid-diaphysis of the femur were used to perform three-dimensional histomorphometric analysis of cortical bone. For cortical bone, the ROI selected for analysis was 10 % of the femoral length in the mid-diaphysis of the femur to determine cortical thickness (Ct.Th), periosteal perimeter (Ps.Pm), and endosteal perimeter (Es.Pm).

### Histochemistry

Histochemistry was performed as previously described [16]. Briefly, femurs were harvested from mice after euthanasia, fixed in 10 % formalin for 24 h, and decalcified in 10 % ethylenediaminetetraacetic acid for 14 days, before being embedded in paraffin. Four-micrometer-thick longitudinally-oriented bone sections were stained with hematoxylin-eosin, TRAP, and toluidine blue to quantify

the number and surface of osteoblasts, the number and surface of osteoclasts, and the number and area of adipocytes, respectively.

OsteoMeasureXP Software (OsteoMetrics, Inc.) was used to perform histomorphometric measurements of two-dimensional parameters of trabecular bones. To label the mineralization fronts, mice were injected with 25 mg/kg calcein at 8 and 2 days before euthanasia. The femurs were fixed in 70 % ethanol, dehydrated in increasing concentrations of ethanol, and the undecalcified bones were embedded in methyl methacrylate. Serial 5- $\mu$ m sections of the femur were made using a microtome. The parameters measured for bone formation were bone formation rate per bone surface (BFR/BS), osteoblast surface per bone surface (Ob.S/BS), and osteoblast number per bone perimeter (N.Ob/B.Pm). The parameters measured for bone resorption were osteoclast surface per bone surface (Oc.S/BS) and osteoclast number per bone perimeter (N.Oc/B.Pm).

### Immunohistochemical Staining

Immunohistochemical staining was performed as previously described [16, 20]. Briefly, bone sections were processed for antigen retrieval by digestion with 0.05 % trypsin at 37 °C for 15 min, and then incubated with a primary anti-OCN antibody (Takara, Japan) overnight at 4 °C. Subsequently, a horseradish peroxidase-streptavidin detection system (Dako) was used to detect the immunoactivity, followed by counterstaining with hematoxylin (Sigma). Sections incubated with polyclonal rabbit IgG (R&D Systems) served as negative controls.

### Western Blot Analysis

Western blotting was performed as previously described [16]. Total cell lysates were separated by sodium dodecyl sulfate polyacrylamide gel electrophoresis and blotted on polyvinylidene difluoride membranes (Millipore). The membranes were incubated with specific antibodies to phospho-Smad2 (Ser465/467) (pSMAD2) (MA5-15122 1; Thermo Scientific), phospho-Smad3 (Ser423/425) (pSMAD3) (9520S; Cell Signaling), SMAD2/3 (3102; Cell Signaling), Runx2 (ab23981; Abcam), or  $\beta$ -actin (ab3280; Abcam), then reprobed with appropriate horseradish peroxidase-conjugated secondary antibodies. Blots were developed using an ECL Kit (Santa Cruz), and exposed to X-ray films.

### Quantitative Reverse-Transcription Polymerase Chain Reaction (qRT-PCR) Analysis

We performed qRT-PCR using a Roche Molecular Light Cycler as previously described [16]. Total RNA from

cultured cells was isolated using the TRIzol reagent (Invitrogen), and reverse transcription was performed using 1 µg total RNA and Superscript II (Invitrogen). Amplification reactions were set up in 25-µL reaction volumes containing SYBR Green PCR Master Mix (PE Applied Biosystems) and amplification primers. One microliter of cDNA was used in each amplification reaction. Primer sequences are listed in Table 1.

### Study Approval

All animal care protocols and experiments were reviewed and approved by the Animal Care and Use Committee of the Laboratory Animal Research Center at Xiangya Medical School of Central South University (Changsha, Hunan, China). All mice were maintained in a specific pathogen-free facility in the Laboratory Animal Research Center at Central South University.

### Statistical Analysis

Data are presented as mean ± standard deviation (SD). Comparisons were made using one-way analysis of variance. Correlations between GDF11 and age were made using Pearson's correlation analysis. All experiments were repeated at least three times, and representative experiments are shown. Differences were considered significant at \* $P < 0.05$ , \*\* $P < 0.01$ .

## Results

### GDF11 Inhibition of Osteoblastic Differentiation of BMSCs

To observe the effect of GDF11 on the osteogenic differentiation of BMSCs, ALP activity and OCN secretion were detected. The results showed that 3–30 ng/mL rGDF11 inhibited ALP activity and OCN secretion (Fig. 1a, b). In addition, to observe the effect of GDF11 on mineralization of BMSCs, Alizarin Red staining was performed. Cells treated with 30 ng/mL rGDF11 showed reduced

mineralization compared with the control (Fig. 1c). We analyzed mRNA levels of Osterix and Runx2 using qRT-PCR, and the results showed that GDF11 dose-dependently inhibited Osterix and Runx2 mRNA expression in BMSCs (Fig. 1d–e). These results showed that GDF11 inhibited osteoblastic differentiation of BMSCs.

### GDF11 had no Significant Effect on Osteoclast Differentiation

Osteoclast formation was investigated after treatment of monocytes and macrophages from bone marrow with M-CSF and RANKL for 8 days. Nuclear factor of activated T-cells cytoplasmic (NFATc1) and TRAP was used as reliable markers of osteoclasts [16, 17]. Our results showed that after treatment with 3–30 ng/mL GDF11, TRAP activity expression and NFATc1 expression were unchanged in multinucleated giant cells (Fig. 2a–c). We also analyzed C-terminal cross-linked telopeptides of type 1 collagen (CTX) by enzyme-linked immunosorbent assay, and the result showed that 3–30 ng/mL rGDF11 did not significantly affect osteoclast differentiation (Fig. 2d). These results all showed that GDF11 did not significantly affect osteoclast differentiation.

### GDF11 Inhibited Bone Formation and Accelerated Age-Related Bone Loss in Mice

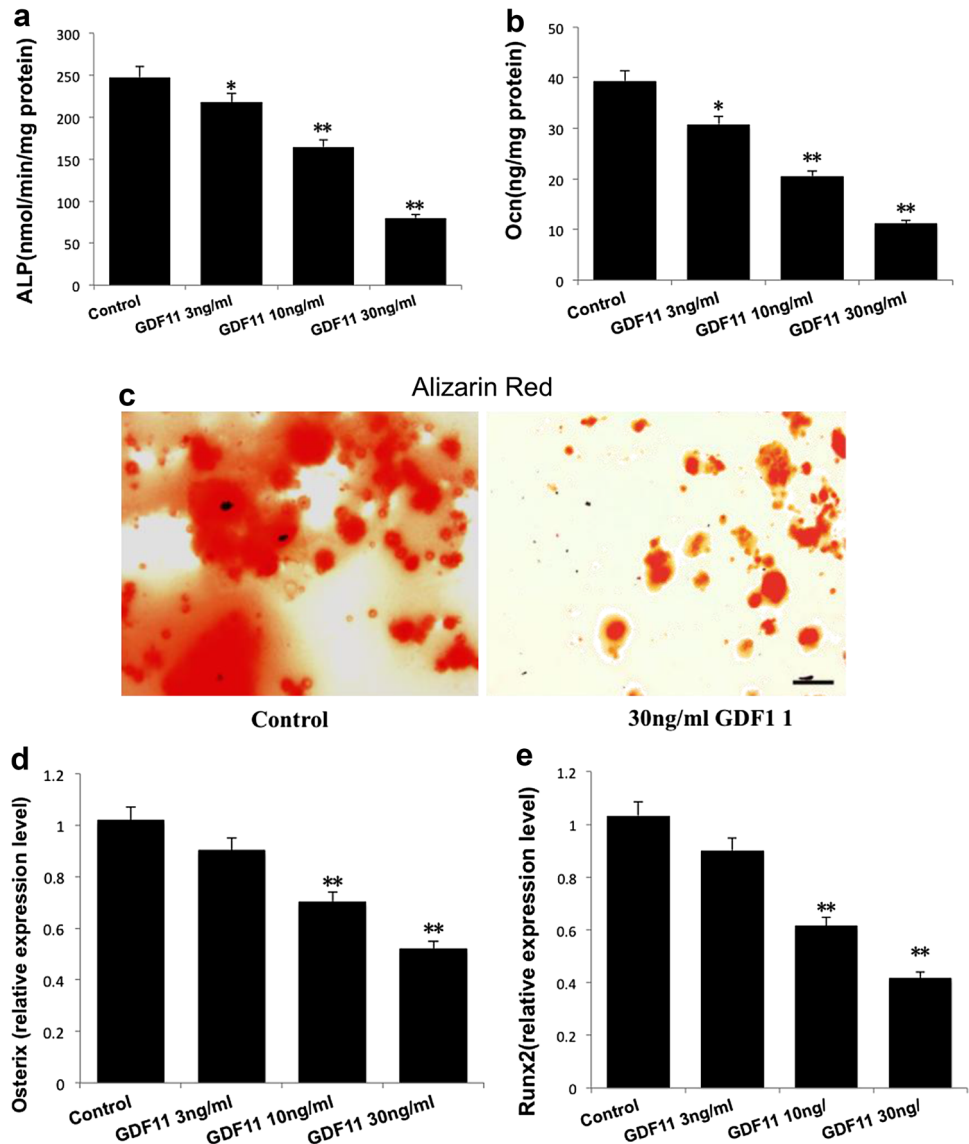
To investigate the role of GDF11 in vivo, the trabecular morphometric parameters and microarchitectural properties of the femur were analyzed by µCT. The trabecular bone volume and number were lower and the trabecular separation was higher in the femurs of mice treated with GDF11 relative to the control (Fig. 3a–e). The cortical bone thickness was lower, and the endosteal Es.Pm was higher in the femurs of mice treated with GDF11 compared with the control (Fig. 3f–h). The trabecular bone formation rates per bone surface (BFR/BS) and mineral apposition rate (MAR) were lower compared with the control (Fig. 3i–j). For Es and Ps bone, quantification of bone formation rate per bone surface (BFR/BS), MAR, and mineralizing surface (MS/BS) was lower in mice treated

**Table 1** Nucleotide sequences of primers used for quantitative RT-PCR detection for mRNA

Gene	Acc. No	Primer sequence(5'to3')	Size
Runx2 (mouse)	NM_001146038	F: ACTTCCTGTGCTCCGTGCTG	20
		R: TCGTTGAACCTGGCTACTTGG	21
Osterix (mouse)	NM_130458	F: ACCAGGTCCAGGCAACAC	18
		R: GCAAAGTCAGATGGGTAAGTAG	22
β-actin (mouse)	NM_007393	F: CTGTCCCTGTATGCCTCTG	19
		R: TGATGTCACGCACGATTT	18

F forward primer, R reverse primer, Acc. No Genbank accession numbers, Size primer size

**Fig. 1** Growth differentiation factor 11 (GDF11) inhibited the osteoblastic differentiation of bone marrow mesenchymal stem cells (BMSCs). BMSCs were cultured in osteogenesis induction medium for 3 days and then treated with 3–30 ng/mL GDF11 for 48 h. **a** Analysis of alkaline phosphatase (ALP) activity and **b** OCN secretion in BMSCs. **c** Representative images of Alizarin Red S staining of matrix mineralization in BMSCs treated with 30 ng/mL GDF11, in osteogenesis induction medium for 21 days. Scale bar 100  $\mu$ m. Quantitative reverse-transcription polymerase chain reaction analysis of the relative levels of osterix (**d**) and Runx2 (**e**) mRNA expression in BMSCs treated with 3–30 ng/mL GDF11 for 48 h.  $n = 5$  per group. Data shown are mean  $\pm$  SD. \* $P < 0.05$ , \*\* $P < 0.01$



with GDF11 compared with the control (Fig. 3k–p). Mice treated with GDF11 had a significantly decreased number and area of osteoblasts on the bone surfaces (Fig. 3q–r) compared with the control.

#### GDF11 had no Significant Effect on Bone Resorption in Mice

The number and area of osteoclasts on the trabecular bone surface were not significantly different in mice treated with GDF11 compared with the control (Fig. 4a–b). No significant difference was observed in CTX levels between the control and GDF11 groups (Fig. 4c). No significant difference was observed in the number and area of adipocytes between the mice treated with GDF11 and the control group (Fig. 4d–e). Together, the results suggest that

intraperitoneal injection of GDF11 inhibited bone formation and decreased bone mass, without affecting bone resorption.

#### GDF11 Inhibited Osteoblast Differentiation by Inducing SMAD2/3 Phosphorylation

To explore the mechanism of the negative regulation of GDF11 on bone formation, while considering the widely recognized roles of the SMAD-Runx2 pathways in the osteogenic differentiation of BMSCs, we investigated the effects of GDF11 on the Smad2/3 phosphorylation and Runx2 expression. Our results showed that GDF11 dose-dependently increased Smad2/3 phosphorylation and decreased the Runx2 expression (Fig. 5a). In addition, pretreatment of BMSCs with the Smad2/3 phosphorylation

inhibitor SB-505,124, prior to GDF11 addition, revealed that Runx2 expression was restored to control levels (Fig. 5b). These results indicate that GDF11 inhibited Runx2 expression by inducing SMAD2/3 phosphorylation, thus suggesting that GDF11 negatively regulates osteogenic differentiation via SMAD2/3 signaling.

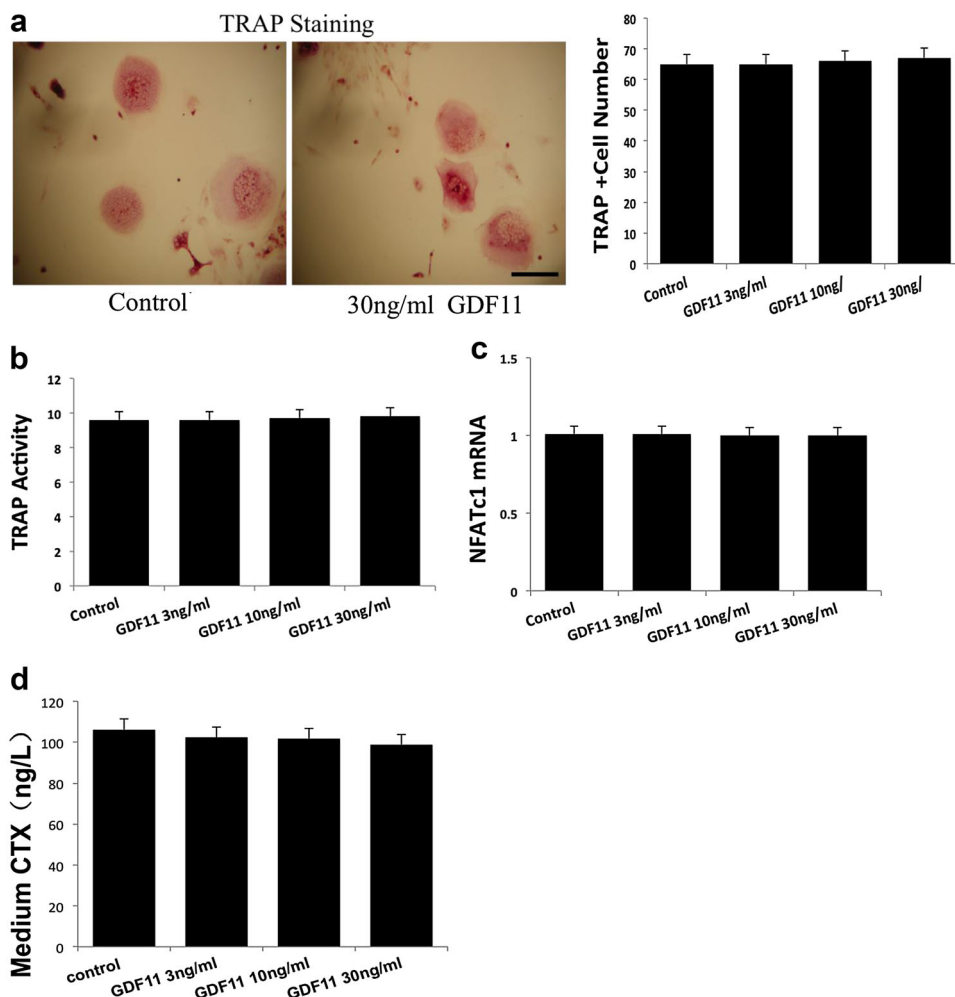
### Discussion

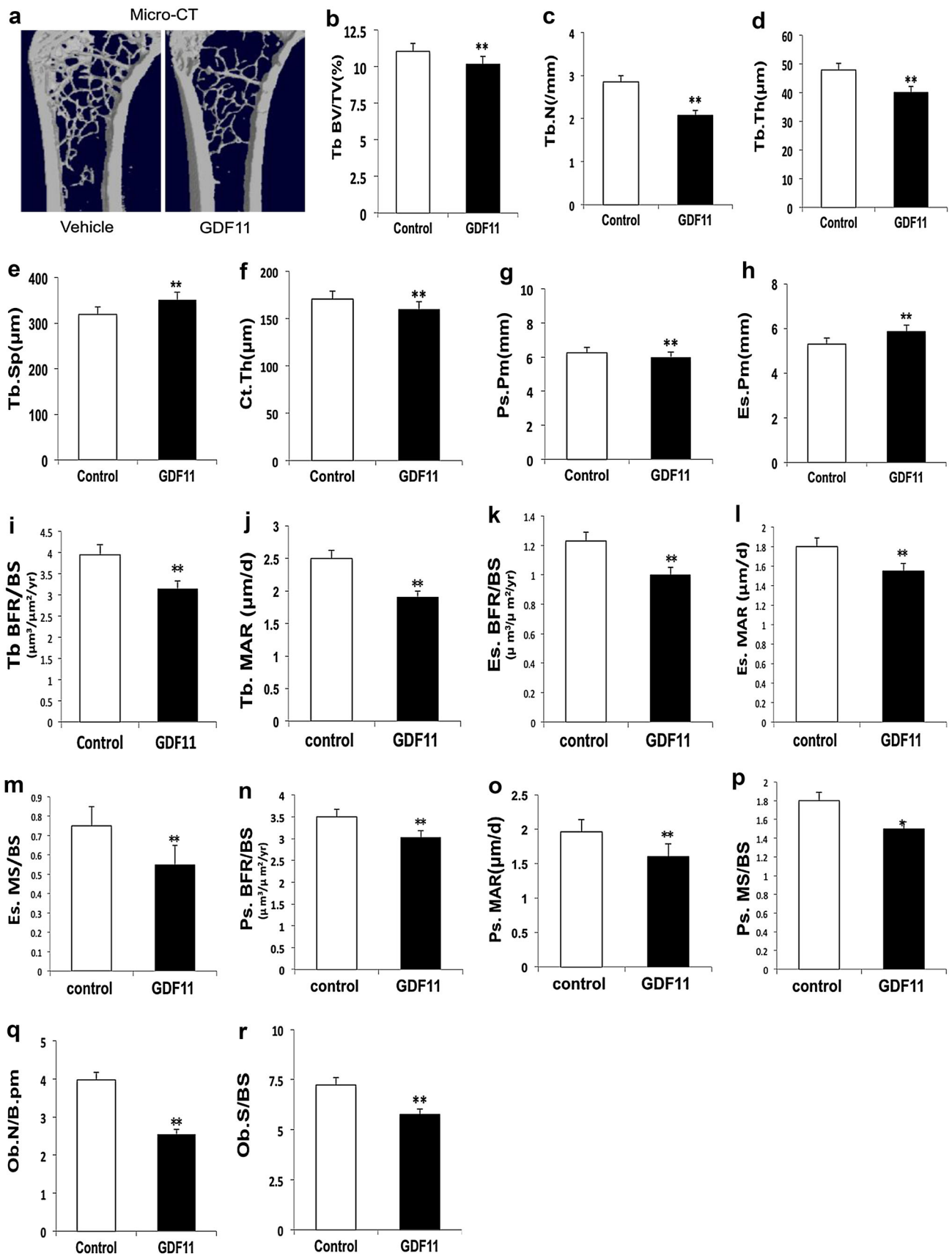
GDF11, a known rejuvenating factor, has become a hotspot of research in recent years. Studies have shown that GDF11 levels decline with aging, which in turn contributes to age-related diseases. Furthermore, the administration of rGDF11 in mice was sufficient to rejuvenate aging organs, such as the heart, muscle, and brain, making them stronger, smarter, and healthier [1, 3, 5]. In contrast, Egerman et al. recently showed that GDF11 increased with age and had negative effects on muscle regeneration and satellite cell expansion [6]. They developed a GDF11-specific immunoassay to detect the GDF11 concentration in the

**Fig. 3** Mice treated with growth differentiation factor 11 (GDF11) mice exhibit decreased bone formation and accelerated bone loss. Twelve-month-old mice ( $n = 6$  per group) were injected intraperitoneally with control or GDF11 (0.1 mg/kg) for 12 weeks. **a–h** Representative microcomputed tomography images (**a**) and quantitative analysis of trabecular (**b–e**) and cortical (**f–h**) bone microarchitectures of mice femurs. (**l–j**) Quantitative data of trabecular of bone formation rates per bone surface (BFR/BS) and mineral apposition rate (MAR) of mice femurs. (**k–p**) Quantification of endosteum of bone formation rates per bone surface (BFR/BS), mineral apposition rate (MAR), and mineralizing surface (MS/BS) of mice femurs. (**q–r**) Osteoblastic parameters were measured using bone morphometric analysis. Number of osteoblasts per bone perimeter (N.Ob/B.Pm); osteoblast surface per bone surface (Ob.S/BS). Tb.BV/TV, trabecular bone volume per tissue volume; Tb.N, trabecular number; Tb.Th, trabecular thickness; Tb.Sp, trabecular separation; Ct.Th, cortical thickness; Ps.Pm, periosteal perimeter; Es.Pm, endosteal perimeter. Data shown are mean  $\pm$  SD. Compared with the control group: \* $P < 0.05$ , \*\* $P < 0.01$

serum of young and older individuals and showed a trend towards increased GDF11 levels in the serum of the older group [6]. Thus, studies investigating the mechanism of action of GDF11 are contradictory. Newer studies of the

**Fig. 2** Growth differentiation factor 11 (GDF11) had no effect on osteoclast differentiation. **a** After osteoclast differentiation was induced with M-CSF and RANKL for 8 days, representative microscopic views of tartrate-resistant acid phosphatase-positive (TRAP<sup>+</sup>) osteoclast formation and TRAP<sup>+</sup> multinucleated giant cell numbers are shown. **b** TRAP activity in multinucleated giant cells is shown. **c** Nuclear factor of activated T-cells cytoplasmic (NFATc1) mRNA levels was determined using quantitative reverse-transcription polymerase chain reaction analysis and is shown as fold induction relative to  $\beta$ -actin. **d** Concentrations of medium C-terminal cross-linked telopeptides of type 1 collagen (CTX) release from cultures are shown. Data shown are mean  $\pm$  SD





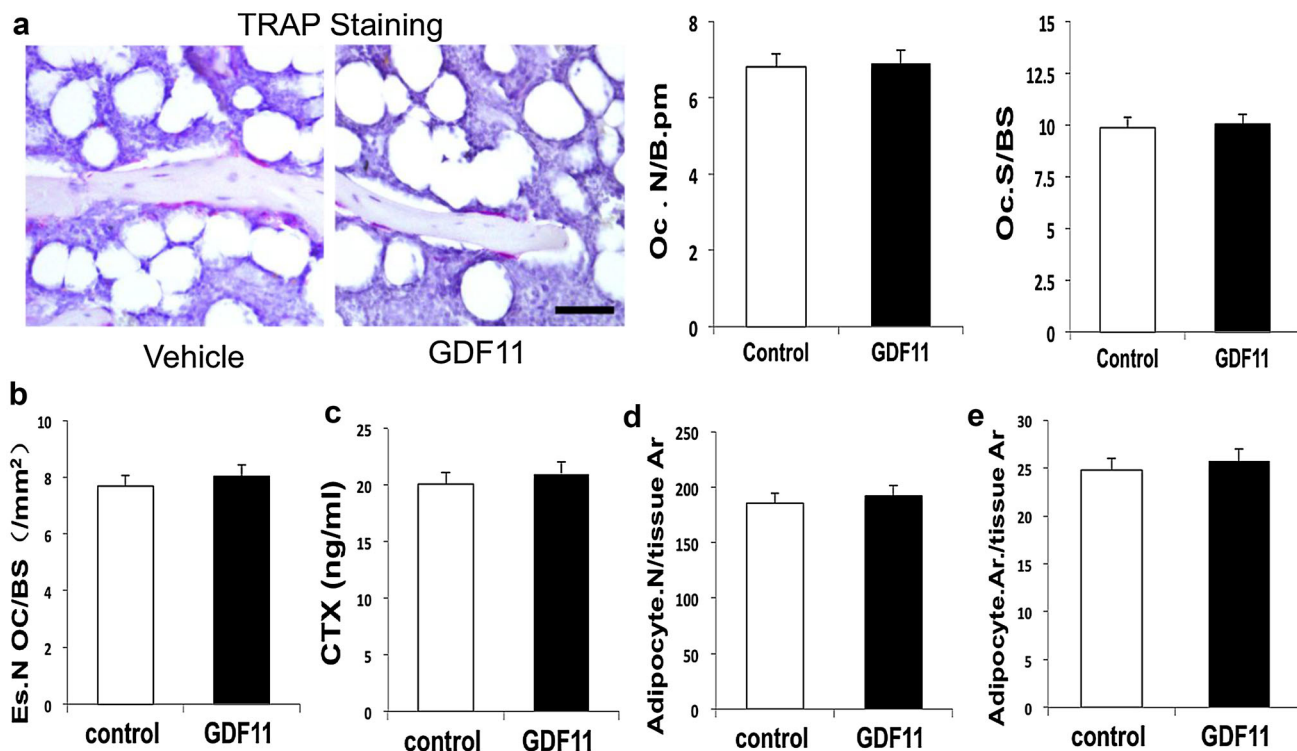


**Fig. 4** Mice treated with growth differentiation factor 11 (GDF11) mice exhibit no effect on bone resorption and adipogenesis. Twelve-month-old mice ( $n = 6$  per group) were injected intraperitoneally with control or GDF11 (0.1 mg/kg) for 12 weeks. **a–b** Representative images of TRAP staining for osteoclastic and bone histomorphometric analysis of mice femurs. *Scale bar 100  $\mu$ m*. Osteoclastic

parameters measured using bone morphometric analysis were N.Oc/B.Pm, Oc.S/BS, and the number of osteoclast cells per endosteal bone surface (*Es.N OC/BS*). **c** C-terminal cross-linked telopeptides of type 1 collagen (*CTX*) levels in mice. **d–e** Quantification of the number and area of adipocytes. Data shown are mean  $\pm$  SD. Compared with the control group: \* $P < 0.05$ , \*\* $P < 0.01$

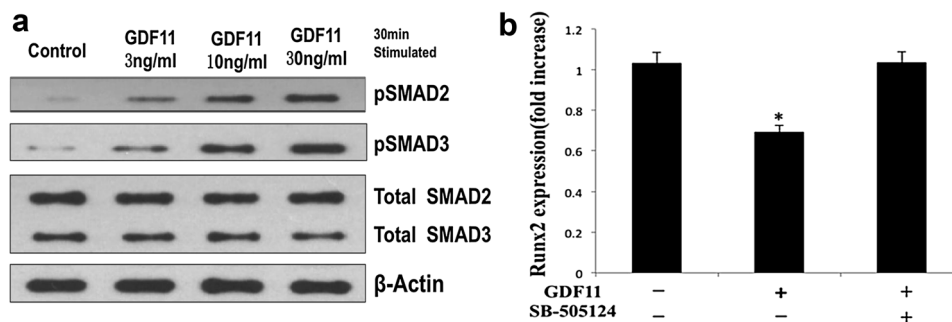


**Fig. 5** Growth differentiation factor 11 (GDF11) inhibited osteoblastic differentiation of bone marrow mesenchymal stem cells (BMSCs) via the SMAD2/3 signal pathway. **a** Western blot analysis revealing GDF11 activation of SMAD signaling. BMSCs were stimulated with control or 3–30 ng/mL GDF11 for 30 min. **b** Quantitative reverse-

transcription polymerase chain reaction analysis detection of Runx2 expression in BMSCs treated with GDF11, without the SMAD2/3 phosphorylation inhibitor SB-505124. Data shown are mean  $\pm$  SD. \* $P < 0.05$

role of GDF11 during aging should be undertaken with a specific antibody for GDF11. In this study, we investigated the effects of GDF11 on bone metabolism in vitro and in vivo. We found that GDF11 inhibited osteoblastic differentiation of BMSCs in vitro and that GDF11 inhibited bone formation and decreased bone mass in mice. We also showed that GDF11 had no effect on osteoclast

differentiation, bone resorption, or adipogenesis. Our study was also contrary to a study by Zhang et al. [11], who showed that GDF11 treatment led to a striking increase in osteoblastogenesis and inhibited adipogenesis from bone marrow mesenchymal stem cells by inhibiting the activity of the peroxisome proliferator-activated receptor- $\gamma$ . We demonstrated that GDF11 inhibited bone formation ex vivo



following the administration of 3–30 g/mL of GDF11 for 48 h, Zhang et al. did not observe similar findings using the different doses of GDF11 (50 µg/mL) over the different periods and different suppliers. Furthermore, Zhang et al. did not perform *in vivo* experiments with GDF11, while our study investigated the effects of GDF11 both *in vitro* and *in vivo*. Therefore, we suggest that attention to dose response and bioactivity is clearly important, as differences in protein refolding and preparation can affect many experiments. Thus, we speculate that differences between our study and that of Zhang et al. could be attributable to variations in commercial protein batches that occurred before rigorous quality control, a combination of different protein sources, protein refolding efficiencies, or concentrations used. However, our *in vivo* study demonstrated that GDF11 inhibited bone formation, and this likely reflects the true scenario *in vivo* more accurately. The findings of Li et al. [15] also support our data, whereby they generated transgenic mice with skeleton-specific overexpression of BMP11 propeptide cDNA, which antagonized GDF11 activity in osteoblasts. These transgenic mice had increased osteoblast activity and enhanced bone formation. Li et al. suggested that inhibition of GDF11 activity stimulated bone formation by increasing osteoblast function. Our results directly showed that the systemic administration of recombinant GDF11 protein inhibited bone formation and induced bone loss *in vivo*.

Then, we investigated the signaling pathway of GDF11. We found that GDF11 inhibited the osteoblastic differentiation of BMSCs via Smad2/3 signaling. Studies have previously shown that GDF11 can activate Smad2/3 phosphorylation in skeletal muscle-derived cells. Smads are key transcription factors of the TGF-β pathway, which form heteromers and translocate into the nucleus to regulate the expression of target genes, such as osteogenic genes [21–23]. Some studies have shown that Smad3 mediated the repressive action of TGF-β on osteoblast differentiation [24]. Chen et al. demonstrated that Smad2 overexpression suppressed Runx2 gene expression in osteoblastic cells [25]. Thus, our study demonstrated that GDF11 induced SMAD2/3 phosphorylation, which led to the inhibition of Runx2 expression. Runx2 is a critical activator of osteogenesis and it induces the expression of bone-related genes. Our results further demonstrated the negative regulation of GDF11 on bone regeneration. We revealed that GDF11 inhibited osteoblastic differentiation via SMAD2/3-Runx2 signaling.

The GDF11 amino acid sequence is 90 % identical to myostatin (GDF8) [1–3]. Previous studies have documented that mice with myostatin deficiency presented with increased bone mass [26–28]. Hamrick et al. demonstrated that loss of myostatin function increases osteogenic differentiation of bone marrow-derived mesenchymal stem

cells, and myostatin-deficient mice showed increased osteogenic differentiation compared with wild-type mice [27–30]. Moreover, studies have demonstrated that GDF11 and myostatin both induce SMAD2/3 phosphorylation, and regulate identical downstream signaling [6]. GDF11 and myostatin similarly inhibited muscle regeneration and decreased satellite cell expansion in mice [6]. It was suggested that GDF11 and myostatin play similar roles in bone metabolism. Thus, we believe that the negative effects of GDF11 on bone mass are convincing.

Finally, we also believe that blockade of GDF11 activity could potentially be a potential therapeutic approach to prevent age-related osteoporosis.

**Acknowledgments** This work was supported by Grant No. 81520108008 from the Major International (Regional) Joint Research Project of China National Natural Scientific Foundation (NSFC), Grant No. 81125006 from the Distinguished Young Scientists of China National Natural Scientific Foundation, Grant No. U1301222 from the NSFC-Guangdong Joint Project, and Grant No. 81570806 from the China National Natural Scientific Foundation.

**Author Contributions** Study design: XHL; Study conduct: QL, MLT, CJL, ZL, TL, and XHL; Data collection: QL, MLT, CJL, and ZL; Data analysis: XHL, QL, MLT, and CJL; Data interpretation: XHL, QL, MLT, CJL, and LZ; Drafting manuscript: XHL, QL, MLT, and CJL; Revising manuscript content: XHL and QL; Approval of the final manuscript: QL, MLT, CJL, ZL, TL and XHL; XHL and QL are primarily responsible for integrity of the data analysis, and all authors take responsibility for and attest to the integrity of the data analysis. XHL is responsible for transmitting the editors' comments to the other authors.

#### Compliance with Ethical Standards

**Conflict of Interest** Xiang-Hang Luo, Qiong Lu, Man-Li Tu, Chang-Jun Li, Li Zhang, Tie-Jian Jiang, and Tang Liu declare that they have no conflict of interest.

**Human and Animal Rights and Informed Consent** Mouse cell line and mice were used in this study. All animal experiments were approved by the Animal Care and Use Committee of the Laboratory Animal Research Center at Xiangya Medical School of Central South University (Changsha, Hunan, China). Strict accordance with the recommendations in the Guide for the Care and Use of Laboratory Animals. No human specimen was used in this study.

#### References

1. Loffredo FS, Steinhauser ML, Jay SM et al (2013) Growth differentiation factor 11 is a circulating factor that reverses age-related cardiac hypertrophy. *Cell* 153:828–839
2. Katsimpardi L, Litterman NK, Schein PA et al (2014) Vascular and neurogenic rejuvenation of the aging mouse brain by young systemic factors. *Science* 344:630–634
3. Sinha M, Jang YC, Oh J et al (2014) Restoring systemic GDF11 levels reverses age-related dysfunction in mouse skeletal muscle. *Science* 344:649–652
4. Smith SC, Zhang X, Zhang X et al (2015) GDF11 does not rescue aging-related pathological hypertrophy. *Circ Res* 117:926–932

5. Mendelsohn AR, Larrick JW (2014) Systemic factors mediate reversible age-associated brain dysfunction. *Rejuvenation Res* 17:525–528
6. Egerman MA, Cadena SM, Gilbert JA et al (2015) GDF11 increases with age and inhibits skeletal muscle regeneration. *Cell Metab* 22:164–174
7. Raisz L (2005) Pathogenesis of osteoporosis: concepts, conflicts, and prospects. *J Clin Invest* 115:3318–3325
8. Ettinger B, Black DM, Nevitt MC et al (1992) Contribution of vertebral deformities to chronic pain and disability. The Study of Osteoporotic Fractures Research Group. *J Bone Miner Res* 7:449–456
9. Cauley JA, Thompson DE, Ensrud KC et al (2000) Risk of mortality following clinical fractures. *Osteoporos Int* 11:556–561
10. Eriksen EF (2010) Cellular mechanisms of bone remodeling. *Rev Endocr Metab Disord* 11:219–227
11. Zhang Y, Shao J, Wang Z et al (2015) Growth differentiation factor 11 is a protective factor for osteoblast genesis by targeting PPAR gamma. *Gene* 557:209–214
12. Shoback D (2007) Update in osteoporosis and metabolic bone disorders. *J Clin Endocrinol Metab* 92:747–753
13. Li H, Xie H, Liu W et al (2009) A novel microRNA targeting HDAC5 regulates osteoblast differentiation in mice and contributes to primary osteoporosis in humans. *J Clin Invest* 119:3666–3677
14. Shim JH, Greenblatt MB, Zou W et al (2013) Schnurri-3 regulates ERK downstream of WNT signaling in osteoblasts. *J Clin Invest* 123:4010–4022
15. Li Z, Kawasumi M, Zhao B et al (2010) Transgenic over-expression of growth differentiation factor 11 propeptide in skeleton results in transformation of the seventh cervical vertebra into a thoracic vertebra. *Mol Reprod Dev* 77:990–997
16. Li CJ, Cheng P, Liang MK et al (2015) MicroRNA-188 regulates age-related switch between osteoblast and adipocyte differentiation. *J Clin Invest* 125:1509–1522
17. Liu Y, Berendsen AD, Jia S et al (2012) Intracellular VEGF regulates the balance between osteoblast and adipocyte differentiation. *J Clin Invest* 122:3101–3113
18. Cao Y, Gomes SA, Rangel EB et al (2015) S-nitrosoglutathione reductase-dependent PPAR $\gamma$  denitrosylation participates in MSC-derived adipogenesis and osteogenesis. *J Clin Invest* 125:1679–1691
19. Nishikawa K, Nakashima T, Takeda S et al (2010) Maf promotes osteoblast differentiation in mice by mediating the age-related switch in mesenchymal cell differentiation. *J Clin Invest* 120:3455–3465
20. Iyer S, Ambrogini E, Bartell SM et al (2013) FOXOs attenuate bone formation by suppressing Wnt signaling. *J Clin Invest* 123:3409–3419
21. Wu MY, Hill CS (2009) TGF $\beta$ —beta superfamily signaling in embryonic development and homeostasis. *Dev Cell* 16:329–343
22. Wu JY, Aarnisalo P, Bastepe M et al (2011) Gs $\alpha$  enhances commitment of mesenchymal progenitors to the osteoblast lineage but restrains osteoblast differentiation in mice. *J Clin Invest* 121:3492–3504
23. Sartori R, Milan G, Patron M et al (2009) Smad2 and 3 transcription factors control muscle mass in adulthood. *Am J Physiol Cell Physiol* 296:C1248–C1257
24. Kang JS, Alliston T, Delston R et al (2005) Repression of Runx2 function by TGF $\beta$  through recruitment of class II histone deacetylases by Smad3. *EMBO J* 24:2543–2555
25. Chen G, Deng C, Li YP et al (2012) TGF $\beta$  and BMP signaling in osteoblast differentiation and bone formation. *Int J Biol Sci* 8:272–288
26. Hamrick MW (2003) Increased bone mineral density in the of GDF8 knockout mice. *Anat Rec A DiscovMol Cell Evol Biol* 272:388–391
27. Hamrick MW, Shi X, Zhang W et al (2007) Loss of myostatin (gdf8) function increases osteogenic differentiation of bone marrow-derived mesenchymal stem cells but the osteogenic effect is ablated with unloading. *Bone* 40:1544–1553
28. Hamrick MW, McPherron AC, Lovejoy CO (2002) Bone mineral content and density in the humerus of adult myostatin-deficient mice. *Calcif Tissue Int* 71:63–68
29. McPherron AC, Lawler AM, Lee SJ (1999) Regulation of anterior/posterior patterning of the axial skeleton by growth differentiation factor 11. *Nat Genet* 22:260–264
30. Hamrick MW, Arounleut P, Kellum E et al (2010) Recombinant myostatin (GDF-8) propeptide enhances the repair and regeneration of both muscle and bone in a model of deep penetrant musculoskeletal injury. *J Trauma* 69:579–583